Monatshefte für Chemie 130, 1031–1045 (1999)

Monatshefte für Chemie
Chemical Monthly

Printed in Austria

Proton Motion and Proton Transfer in the Formic Acid Dimer and in 5,8-Dihydroxy-1,4-naphthoquinone: A PAW Molecular Dynamics Study

Katharina Wolf, Alexandra Simperler, and **Werner Mikenda***

Institut für Organische Chemie, Universität Wien, A-1090 Vienna, Austria

Summary. A molecular dynamics study on proton motion and (double) proton transfer in the formic acid dimer (*FAD*) and in 5,8-dihydroxy-1,4-naphthoquinone (*DHN*) is reported that has been performed with the Projector Augmented Wave method (PAW). PAW trajectories were calculated with a time interval of 0.12 fs, for evolution time periods up to 20 ps, and for temperatures in the range 500–700 K. Two basic situations can be clearly distinguished: normal periods that correspond to normal asymmetric O–H · · O hydrogen bonds, where the proton remains trapped at one oxygen atom, and active periods that correspond to (near-)symmetric O · · H · · O hydrogen bonds, where the proton undergoes large amplitude motions between the two adjacent oxygen atoms. Within the active periods one may distinguish between isolated transitions, where a proton just moves from one to the other oxygen atom, crossing-recrossing events, where a proton moves from one to the other oxygen atom but almost immediately turns back, and shuttling periods, where a proton undergoes several consecutive transitions. Moreover, one may also distinguish between single processes, where only one O–H · · O group is involved, and double processes, where both O–H · · O groups are simultaneously involved. It is shown that a reasonable and descriptive understanding of the active processes can be obtained by considering the time evolution of the potential energy that governs the motion of the proton between the two adjacent oxygen atoms. A main difference between *FAD* and *DHN* concerns the double proton transfer processes. In the first case these are almost exclusively simultaneous one-step processes, whereas in the second case these are mainly two-step processes, *i.e.* two successive single transitions. This difference can be attributed to the fact that with *DHN* a single proton transfer process yields the metastable 4,8-dihydroxy-1,5-naphthoquinone tautomer, whereas with *FAD* single proton transfer does not result in a metastable intermediate.

Keywords. 5,8-Dihydroxy-1,4-naphthoquinone; Formic acid dimer; Molecular dynamics; Projector Augmented Wave method; Proton transfer.

Protonentransfer im Dimer der Ameisensäure und in 5,8-Dihydroxy-1,4-naphthochinon: Eine PAW-Molekulardynamik-Studie

Zusammenfassung. Mit Hilfe der *Projector Augmented Wave*-Methode (PAW) wurden Molekulardynamiksimulationen über die Protonenbewegung und den Protonentransfer im Dimer der

* Corresponding author

Ameisensäure (*FAD*) und in 5,8-Dihydroxy-1,4-naphthochinon (*DHN*) durchgeführt. PAW-Trajektorien wurden mit einem konstanten Zeitintervall von 0.12 fs, über Zeiträume von bis zu 20 ps und für Temperaturen im Bereich 500–700 K berechnet. Zunächst lassen sich zwei grundlegende Situationen unterscheiden: normale Perioden, die einer normalen asymmetrischen O–H · · O-Wasserstoffbrückenbindung entsprechen, bei der das Proton eindeutig an ein Sauerstoffatom gebunden ist, und aktive Perioden, die einer annähernd symmetrischen O · · H · · O-Wasserstoffbrückenbindung entsprechen, bei denen sich das Proton mit deutlich größerer Amplitude zwischen beiden benachbarten Sauerstoffatomen bewegt. Weiters kann man innerhalb der aktiven Perioden zwischen isolierten Übergängen, bei denen das Proton von einem zum anderen Sauerstoff wechselt, *crossing-recrossing*-Prozessen, bei denen sich das Proton ebenfalls von einem zum anderen Sauerstoff bewegt, aber sofort wieder zurückkehrt, und *shuttling*-Perioden, bei denen das Proton mehrere aufeinanderfolgende Übergänge ausführt, unterscheiden. Darüber hinaus läßt sich noch zwischen Einzelprozessen, an denen nur eine O–H · · O Gruppe beteiligt ist, und Doppelprozessen, an denen beide O–H · · O Gruppen gleichzeitig beteiligt sind, differenzieren. Eine physikalisch sinnvolle und anschauliche Erklärung der aktiven Prozesse erreicht man durch die Betrachtung der zeitlichen Entwicklung der potentiellen Energie, die die Bewegung des Protons zwischen den beiden Sauerstoffatomen bestimmt. Soweit Doppel-Protonentransfer-Prozesse betroffen sind, besteht zwischen *FAD* und *DHN* ein auffallender Unterschied. Während diese im ersten Fall fast ausschließlich simultane Einstufenprozesse sind, findet man im zweiten Fall überwiegend Zweistufenprozesse, das heißt, es handelt sich um zwei aufeinanderfolgende Einzelübergänge. Dies läßt sich dadurch erklären, daß bei *DHN* ein einfacher Protonentransfer zu einem metastabilen Zwischenzustand führt (5,8-Dihydroxy-1,4-naphtochinon), was bei *FAD* nicht der Fall ist.

Introduction

Recently, we have reported a Projector Augmented Wave (PAW) [1] molecular dynamics study on proton motion and intramolecular proton transfer in malonaldehyde [2, 3]. PAW is based on the direct molecular dynamics approach of *Car* and *Parrinello* [4], which combines classical dynamics with quantum mechanical forces and which yields full molecular dynamics at finite temperatures on a picosecond time scale. Basically, since all nuclear motions are treated classically, no quantum effects such as proton tunnelling or zero point motion are taken into account. Hence, the PAW calculations establish a high temperature approach for dynamic processes, where quantum phenomena are negligible or at least less important (whereas common quantum mechanical studies that focus on tunnelling effects rather correspond to a low temperature limit approximation). Within the framework of the PAW approach, proton motion in malonaldehyde can reasonably well be understood in terms of the full dynamics of the molecule: at each moment (time step), the potential which governs the proton motion between the two adjacent oxygen atoms, is determined by the current molecular geometry. Three typical situations could be distinguished: (*i*) normal periods, in which the proton remains firmly trapped at one oxygen atom, (*ii*) isolated transitions, where the proton rapidly moves from one to the other oxygen atom, and (*iii*) shuttling transition regions, where several consecutive proton transitions take place.

In the present paper we report PAW molecular dynamics studies on two more complex systems that are capable of double proton transfer processes: the cyclic formic acid dimer (*FAD*) and 5,8-dihydroxy-1,4-naphthoquinone (naphtazarine, *DHN*). *FAD* (Fig. 1) belongs to the most extensively studied model systems for the investigation of hydrogen bonded dimers and of intermolecular double proton

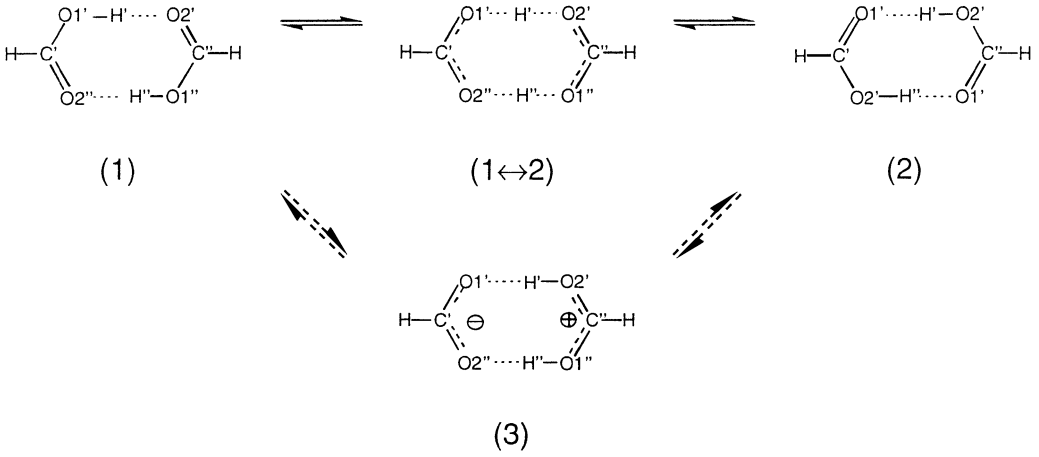

Fig. 1. Prototropic isomers and double proton transfer transition state of the cyclic formic acid dimer (*FAD*)

transfer processes which play an important role in various fields of chemistry and biochemistry. Structural and spectroscopic properties of *FAD* have been the subject of extensive experimental [5–13] and theoretical [14–24] work. Nevertheless, because of problems with the rather complex and poorly resolved spectra, tunnelling splitting in *FAD* has never been observed experimentally so far. According to theoretical studies, double proton transfer in *FAD* most likely takes place by a simultaneous one-step mechanism *via* a D_{2h} symmetric transition state ((*1*)→(*1*↔*2*)→(*2*) in Fig. 1) [25–31].

For *DHN* (Fig. 2), which has been chosen as an example for intramolecular double proton transfer systems, only minor experimental [32–40] and theoretical [41–45] studies are available in the literature. According to IR and laser-induced fluorescence low-temperature matrix isolation investigations [36, 37], the C_{2v} symmetric 5,8-dihydroxy-1,4-naphthoquinone (5,8-*DHN*; (*1*) and (*2*) in Fig. 2) represents the most stable configuration. Recently, the possible isomers of *DHN* and the transition states for proton transfer reactions (Fig. 2) have been theoretically studied at the MP2/6-31G*//HF/6-31G level of theory [41]. According to this study, the C_{2h} symmetric 4,8-dihydroxy-1,5-naphthoquinone (4,8-*DHN*; *(3)* in Fig. 2) is also a (local) energetic minimum ($\Delta E = 37\,\mathrm{kJ \cdot mol^{-1}}$ relative to 5,8-*DHN*), whereas the most probable transition states for a single and for a simultaneous double proton transition with C_s and D_{2h} symmetries, respectively, are saddle points ($\Delta E = 38$ and $53\,\mathrm{kJ \cdot mol^{-1}}$). Based on these results, the authors claimed that double proton transfer processes in *DHN* should rather take place by a two-step mechanism involving the metastable 4,8-*DHN* isomer ((*1*)→(*1*↔*3*)→(*3*)→(*2*↔*3*)→(*2*) in Fig. 2).

In the following sections we give some computational details, present *R*(OH) time evolutions to visualize the results of the PAW calculations and to distinguish between different kinds of proton motion events, show potential energy time evolutions that provide a basis for an understanding of the physical backgrounds of the proton transfer processes, and finally discuss similarities and differences between the two title compounds.

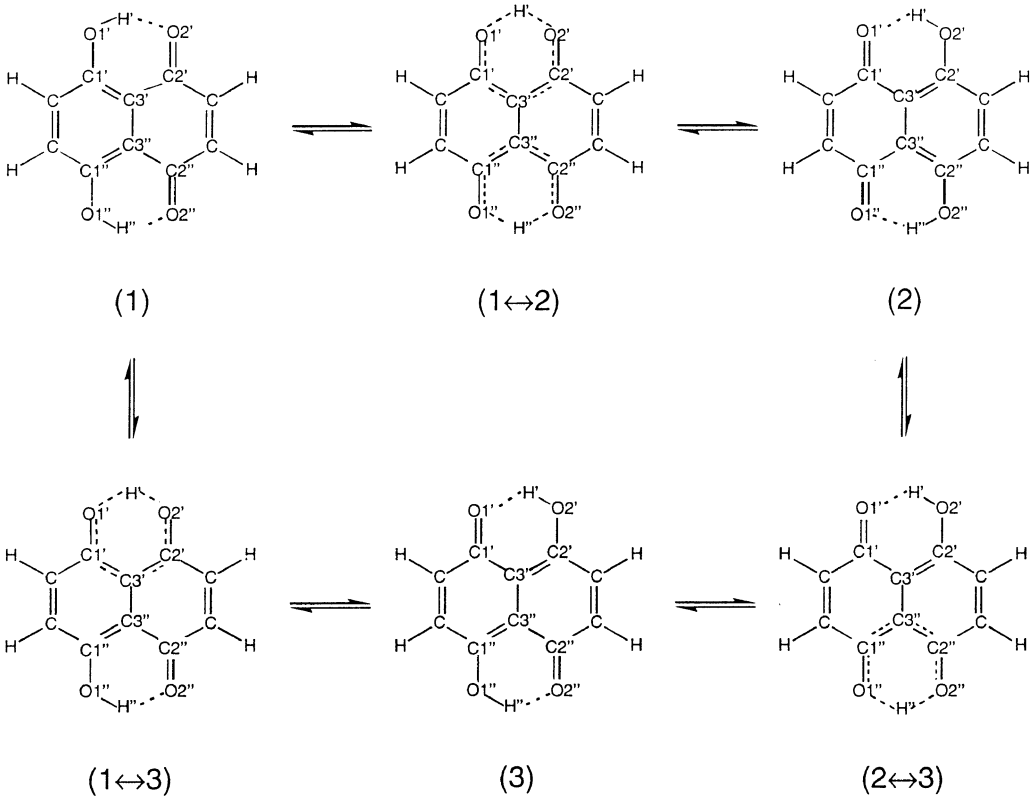

Fig. 2. Prototropic isomers and proton transfer transition states of dihydroxy-naphthoquinone (*DHN*)

Methods

The PAW molecular dynamics simulations were performed for evolution time periods up to 20 ps with constant time intervals of 0.1209 fs (5 a.u.). The temperature of the molecular dynamics runs (between 500 K and 800 K) was controlled with the *Nosè-Hoover* thermostat [46, 47]. *Perdew* and *Zunger's* [48] parametrization of the density functional, based on the results of *Ceperley* and *Alder* [49], was used, and the generalized gradient corrections of *Becke* [50] and *Perdew* [51] were applied. The basis set included plane waves with a cutoff of 30 Ry ($=39.4\,\mathrm{kJ\cdot mol^{-1}}$); the electron density was represented with a cutoff of 60 Ry. The plane waves were augmented with *s*-type projector functions for hydrogen atoms and with *s*-, *p*-, and *d*-type projectors for carbon and oxygen atoms. For a comparison of the performance of the PAW calculations with other more common quantum chemical methods, geometry optimizations were performed with the Gaussian92 [52] programs at several levels of theory using the 6-31G(d,p) basis set throughout. Selected geometric and energetic data are compiled in Tables 1 and 2 along with the corresponding zero temperature PAW values. Tables 1 and 2 indicate that the hydrogen bond strengths may be slightly overestimated by the PAW calculations and that our proton transfer barrier heights may be somewhat too low. Since we are exclusively dealing with qualitative features and with a qualitative picture of the proton transfer processes at finite temperatures, the accuracy should be sufficient. What is more, we find a very good agreement between the experimental and the PAW calculated ν(OH) frequencies (see below) which gives strong evidence that our force fields should indeed be realistic.

Table 1. Selected bond distances (pm) and angles (°), and proton transfer barriers ΔE(kJ · mol^{-1}) of *FAD* as obtained from experimental and theoretical data

	exp[a]	HF[b]	MP2[b]	B3LYP[b]	B3P86[b]	PAW
(*1*)						
O–H	1.036	96.3	99.4	100.7	101.5	106.8
H · · O	1.667	183.1	171.2	164.4	157.6	143.4
O · · · O	2.703	278.9	270.5	265.0	259.1	250.2
O–H · · O	180	174	179	179	180	180
C–O	1.323	129.8	132.0	131.0	130.1	129.9
C=O	1.220	119.6	123.0	122.6	122.7	124.0
C · · · C		340.3	383.5	377.7	371.5	364.5
(1↔2)						
H · · O		118.8	120.5	121.0	120.4	122.5
O · · · O		237.6	240.9	241.9	240.8	244.9
O–H · · O		179	178	179	178	177
C⋯O		124.2	126.9	126.5	126.1	127.0
C · · · C		349.9	353.7	354.6	353.3	359.0
$\Delta E = E(1\leftrightarrow 2) - E(1)$	80.1[c]	69.6	34.3	22.5	15.6	8.9

[a] Geometric data from electron diffraction measurements[13]; [b]6–31G(d,p) basis set; [c]estimated from NIR measurements of ν(O–H) overtone bands [12]

Table 2. Selected bond distances (pm) and angles (°), and proton transfer barriers ΔE(kJ · mol^{-1}) of *DHN* as obtained from theoretical data

	HF[a]	MP2[a]	B3LYP[a]	B3P86[a]	PAW
(*1*)					
O–H	95.2	98.7	0.99.6	100.1	102.9
H · · O	184.3	172.0	1.67.7	1.63.1	167.1
O · · · O	264.6	260.8	2.57.7	254.6	261.3
O–H · · · O	140	148	148	150	151
C–O	133.0	134.5	1.33.6	132.7	134.2
C=O	120.7	125.4	1.24.9	124.7	126.6
C · · · C	247.3	248.2	2.47.7	246.4	249.8
(*3*)					
O–H	95.9	101.0	101.8	103.0	104.5
H · · O	179.7	159.9	157.9	151.6	163.1
O · · · O	261.9	253.3	252.1	248.0	259.9
O–H · · O	142	152	151	153	152
C–O	131.4	132.8	132.2	131.3	133.6
C=O	121.7	126.7	126.1	126.0	127.1
C · · · C	244.2	246.1	245.9	244.6	249.2
$\Delta E = E(3) - E(1)$	43.8	29.5	19.1	16.5	13.1
$\Delta E = E(1\leftrightarrow 3) - E(1)$	67.6	31.6	21.5	16.9	16.0
$\Delta E = E(1\leftrightarrow 2) - E(1)$	125.5	49.0	35.1	26.3	20.0

[a] 6–31G(d,p) basis set

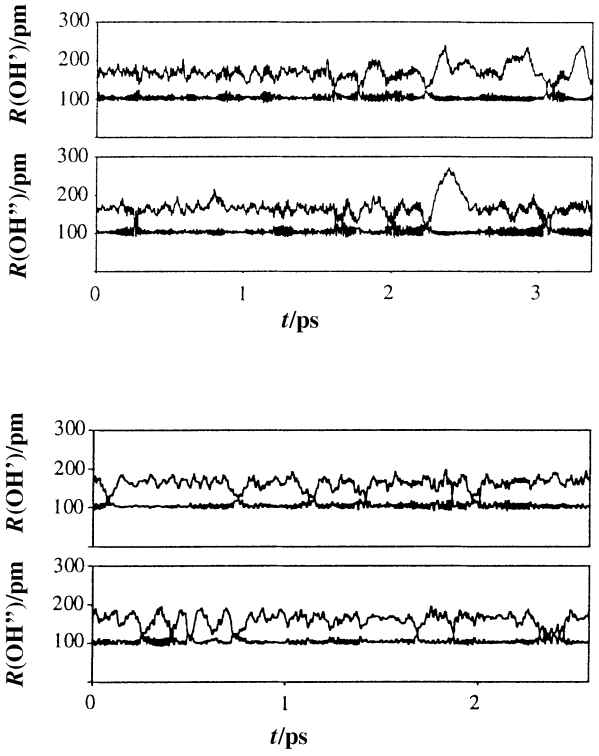

Fig. 3. Time evolutions of the R(OH) distances of *FAD* (top) and *DHN* (bottom)

Results and Discussion

PAW trajectories

In Fig. 3, selected cuts of time evolutions of the two $R(\mathrm{OH}')$ and the two $R(\mathrm{OH}'')$ distances are shown for *FAD* (time period: 3.4 ps, temperature: 700 K) and for *DHN* (time period: 2.7 ps, temperature: 500 K). At first glance one can clearly distinguish between two fundamental situations: normal periods, where the two R(OH) trajectories are well separated from each other (see also Fig. 4a), and active periods, where the two R(OH) trajectories show one or more cross over points (see also Figs. 4b–h). Within the normal periods the proton remains trapped at one oxygen atom and undergoes a stationary motion that corresponds to the ν(OH) stretching mode of a normal, clearly asymmetric O–H $\cdots$ O hydrogen bond. The vibrational amplitude is typically 100 pm, and the average frequencies are 80 THz and 84 THz (2800 and 2700 cm^{-1}) for *FAD* and *DHN*, respectively. In contrast, within the active periods the proton undergoes large amplitude motions between the two adjacent oxygen atoms, with an amplitude of typically about 300 pm.

Closer inspection of the trajectories reveals that the processes within the active periods are largely variable, stochastic events. Selected examples are shown in Fig. 4 by blow-ups of the time evolutions of the $R(\mathrm{OH}')$ and $R(\mathrm{OH}'')$ distances. For a phenomenological description, to a first approximation the active periods can be classified according to two main criteria. First, according to the number of cross-

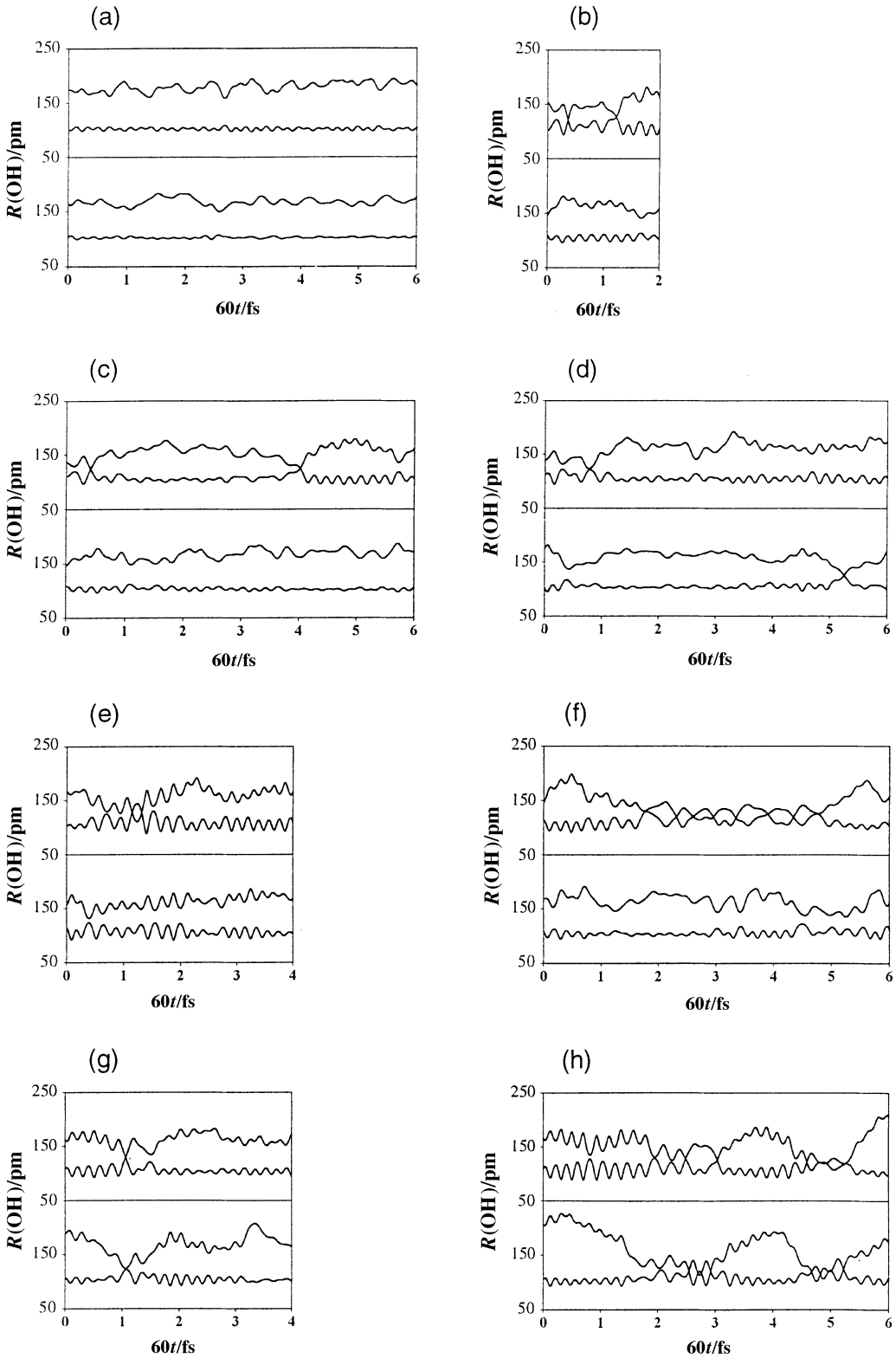

Fig. 4. Time evolutions of the R(OH) distances showing (a) a normal period (*DHN*), (b) a consecutive single proton transfer process (*DHN*), (c) a successive single proton transfer process (*DHN*), (d) a successive double proton transfer process (*DHN*), (e) a single concerted crossing-recrossing event (*DHN*), (f) a single proton shuttling period (*DHN*), (g) a simultaneous double proton transfer (*FAD*), and (h) a double proton shuttling period (*FAD*)

over points we can distinguish between (*i*) isolated proton transfer processes (Figs. 4b–d,g) where the proton just moves from one to the other oxygen atom (one cross over point, O–H$\cdot\cdot$O$\rightarrow$O$\cdot\cdot$H–O), (*ii*) crossing-recrossing processes (Fig. 4e) where the proton moves from one to the other oxygen atom but almost immediately goes back to the first oxygen (two cross over points, O–H$\cdot\cdot$O$\rightarrow$O$\cdot\cdot$H–O$\rightarrow$O–H$\cdot\cdot$O), and (*iii*) shuttling periods (Figs. 4f, h), where the proton undergoes several consecutive transitions (three or more cross over points, O–H$\cdot\cdot$O$\rightarrow$O$\cdot\cdot$H–O$\rightarrow$ O–H$\cdot\cdot$O$\rightarrow$O$\cdot\cdot$H–O$\rightarrow\rightarrow$). Second, according to the number of O–H$\cdot\cdot$H groups that are simultaneously active we can distinguish between (*i*) single processes (Figs. 4b–f) where only one O–H$\cdot\cdot$O group is involved and (*ii*) double processes (Figs. 4g–h) where both O–H$\cdot\cdot$O groups are simultaneously involved. To be sure, these classifications are neither unambiguous nor do they account for the full variety of the observed processes, but they provide a reasonable basis for the following discussions.

Geometric considerations

In a foregoing study on malonaldehyde [2–3] it has been shown that from a geometrical point of view normal and active periods are mainly characterized by long and short R(O$\cdot\cdot$O) distances, respectively, although there exists no well defined borderline which could serve as a necessary or a sufficient criterion for a clear cut distinction. The very same is true for *FAD* and *DHN*: the average R(O$\cdot\cdot$O) distances within the normal regions amount to 272 pm and 263 pm, whereas the average R(O$\cdot\cdot$O) distances of the cross-over points are 248 pm and 239 pm, respectively. From an analysis of the geometric data by statistical methods, several additional geometric parameters could also be determined which on average show more or less systematic differences between normal and active periods. In summary, however, it is not possible to reliably discriminate between normal periods and (cross-over points of) active periods by purely geometric arguments, *i.e*. there are no definite requirements for activity to take place, and the individual active periods may be associated with largely different geometries.

Energetic considerations

Previously it has been shown [2–3] that a reasonable and descriptive understanding of the driving forces that govern the motion of the proton between the two adjacent oxygen atoms can be obtained by considering potential energy time evolutions ($E(\rho, t)$). Some selected examples are shown in Figs. 5–7 by staggered plots of consecutive ($\Delta t = 2.4$ fs) potentials $E(\rho)_t$. The single potentials $E(\rho)_t$ (*i.e*. the single time frames) were calculated by taking the corresponding PAW geometries, fixing all atoms (except the proton under consideration), moving the proton stepwise along a proper proton transfer reaction coordinate, $\rho = (R(\mathrm{O1H}) \cdot \cos\theta(\mathrm{O2O1H}))/R(\mathrm{O1O2})$, and optimizing the proton position at each step. The potential $E(\rho)_t$ obtained by such a point to point calculation represents the energetic precondition for a hypothetical, infinitely rapid proton transfer for the molecular geometry just given at that time step. Finally, the complete potential energy time evolution $E(\rho,t)$ (*i.e*. the staggered plots) illustrates the energetic situation as experienced by the

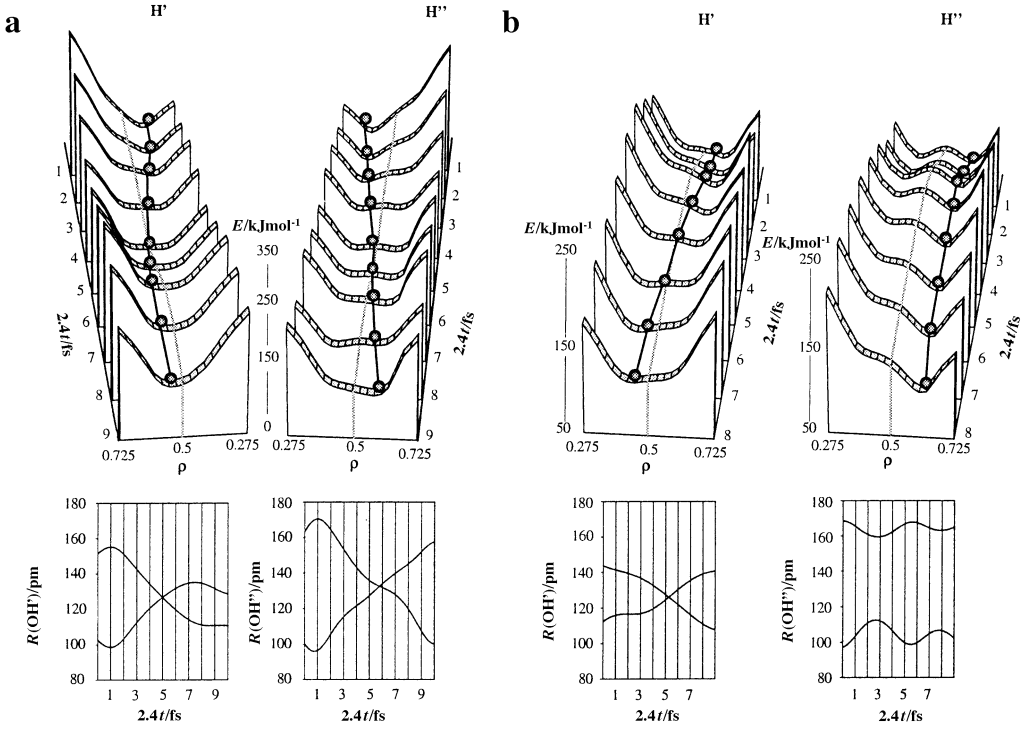

Fig. 5. Time evolutions of $E(\rho)$ potentials (time interval between consecutive frames: 2.42 fs; the circles indicate the actual proton positions) and corresponding time evolutions of the R(OH) distances for (a) an isolated double proton transfer process (*FAD*) and for (b) an isolated single proton transfer process (*DHN*)

proton on the fly which permanently changes due to the dynamically changing molecular geometry. In Figs. 5–7, such potential energy time evolutions $E(\rho,t)$ are shown by pairs of staggered plots ($\Delta t = 2.4$ fs) along with the actual proton motions as obtained from the PAW trajectories (indicated by circles). Additionally, the time evolutions of the R(OH) distances are shown; each vertical line corresponds to the equally numbered time frame of the plot.

Figures 5a and 5b show nine and eight snapshots (total time periods: 19.2 and 16.8 fs) of an isolated double proton transfer process in *FAD* and of an isolated single proton transfer process in *DHN*, respectively. The time evolutions $E(\rho, t)$ for the active protons (H′ and H″ for *FAD*, H′ for *DHN*) start with normal, strongly asymmetric potentials, whose minima are located at one oxygen atom; then they change to broad, (near-)symmetric single-minimum or shallow double-minimum potentials, and end with again strongly asymmetric potentials with the minima now being located at the other oxygen atom. As to the protons, at the beginning they are firmly attached to one oxygen atom; then, following the $E(\rho, t)$ gradient, they rapidly move towards the other oxygen, where they finally remain trapped.

Figure 6a shows 21 snapshots (48 fs) of a double proton shuttling period in *FAD*, Fig. 6b shows 15 snapshots (33.6 fs) of a single proton shuttling period in *DHN*. Like isolated processes, shuttling periods are also associated with broad, (near-)symmetric single-minimum or shallow double-minimum potentials. The

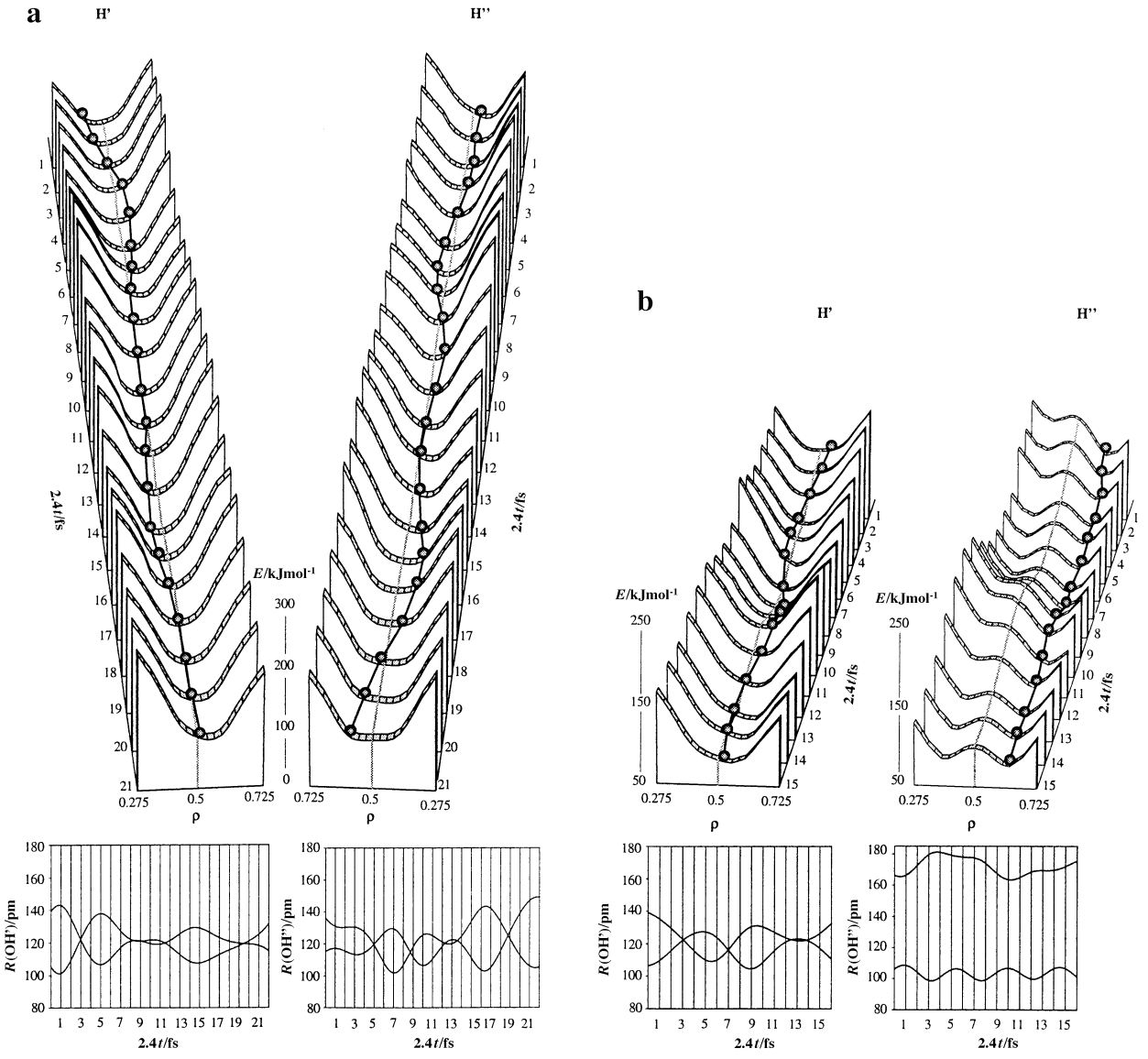

Fig. 6. Time evolutions of $E(\rho)$ potentials (time interval between consecutive frames: 2.42 fs; the circles indicate the actual proton positions) and corresponding time evolutions of the R(OH) distances for (a) a double proton shuttling period (*FAD*) and for (b) a single proton shuttling period (*DHN*)

main difference is that in the first case the normal asymmetric potential is readily re-established, whereas in the latter case the abnormal (near-)symmetric potential persists for a longer time period, thus leading to the observed large-amplitude proton motions. In Fig. 7, as a final example, an outstanding crossing-recrossing process in *FAD* is shown (10 snapshots, 21.6 fs) where the potential remains clearly asymmetric during the whole period. In this case the observed large amplitude proton motion obviously results from an accidental, exceptionally large kinetic energy of the proton, as already indicated by the abnormal large elongation in

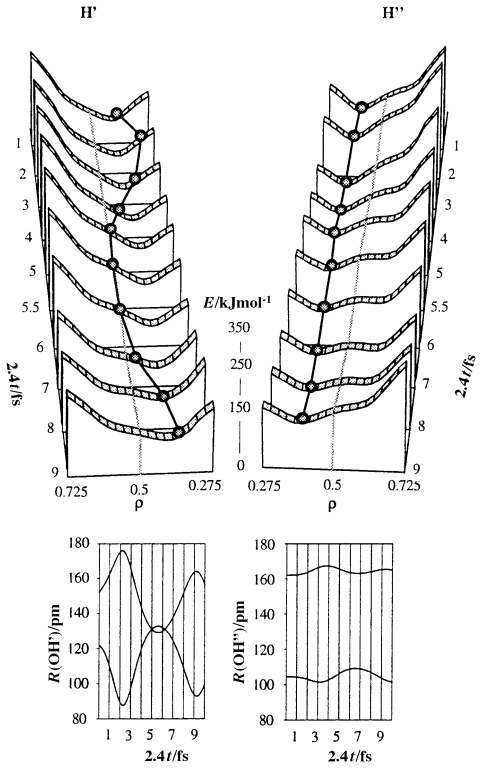

Fig. 7. Time evolutions of $E(\rho)$ potentials (time interval between consecutive frames: 2.42 fs; the circles indicate the actual proton positions) and corresponding time evolutions of the R(OH) distances for a crossing-recrossing process (*FAD*)

frame 2. This clearly shows that the proton motion is not only governed by the potential $E(\rho, t)$, but also by kinetic factors, *i.e.* by the proton's momentum.

From the above discussion, the physical backgrounds of the proton motion, as obtained by the PAW calculations, may be summarized as follows. (*i*) At any given time step, the potential energy $E(\rho)_t$ that governs the proton motion between the two adjacent oxygen atoms is determined by the current molecular geometry, which on its part is determined by the full dynamics of the molecule. Basically, the proton motion is not rigorously determined, but (only) governed by the potential $E(\rho)_t$, since the actual motion also depends on the current kinetic energy (the momentum) of the proton. (*ii*) On average, the normal periods correspond to normal, clearly asymmetric O–H$\cdot\cdot$O hydrogen bonds, *i.e.* the average geometries are similar to those of the stable isomers of the two compounds – (*1*) and (*2*) – and $E(\rho)_t$ is an asymmetric potential with the minimum clearly located at one of the two oxygen atoms in which the proton undergoes a normal ν(O–H) stretching vibration. (*iii*) On the other hand, on average the active periods correspond to (near-)symmetric O$\cdot\cdot$H$\cdot\cdot$O hydrogen bonds, *i.e.* the average geometries are similar to those of the proton transfer transition states of the two compounds – (*1*↔*2*), (*1*↔*3*), and (*2*↔*3*) – and $E(\rho)_t$ is a broad, (near-)symmetric single- or double-minimum potential in which the proton can undergo large amplitude

motions between the two adjacent oxygen atoms. This motion rather corresponds to a quasi-stationary $\nu(O\cdot\cdot H\cdot\cdot O)$ stretching vibration than to consecutive single proton transfers.

FAD versus DHN

Based on the above classification and on the physical backgrounds of active processes, we finally focus on similarities and/or differences between the two title compounds. With *FAD* we mainly find two different situations (about 90%), isolated double proton transfer processes and single crossing-recrossing processes, whereas double and single proton shuttling periods are rather scarce (about 10%) and single proton transfer processes are totally absent. For the double proton transfer processes (Fig. 4g), the delay between the two proton motions, as measured by the difference between the two cross-over points, ranges from 0.1 to 11 fs, which gives justification to talk about simultaneous or concerted one-step processes (note that 12 fs corresponds to a normal ν(OH) vibrational cycle). Similarly, the crossing-recrossing events (Fig. 4e) are also concerted one-step processes; the differences between the two cross over points are less than 12 fs in all instances.

With *DHN* the situation is largely different and distinctly more complex. First of all, simultaneous processes, *i.e.* double proton transfers and double proton shuttling periods, are rather scarce (< 15%). Second, similar to *FAD* single proton crossing-recrossing (Figs. 4b, c) comprises about 40% of the active periods; however, the differences between the two cross-over points range typically from 10 to 30 fs, *i.e.* most of them are distinctly larger than with *FAD*, and in an extreme case we found a delay of as much as 220 fs. This means that with *DHN* crossing-recrossing not only takes place as clear cut concerted one-step process, as is the case with *FAD*, but also as successive two-step process (with many additional cases in-between). Consistently, we also find successive two-step double proton transfer processes (> 10%); they start with an isolated single proton transition at one O–H$\cdot\cdot$O group followed by a second isolated proton transition at the other O–H$\cdot\cdot$O group (Fig. 4d). Quite noticeable, the delay between the two transitions is always rather large; it ranges from 30 to 270 fs. Finally, the remaining 25% of the active periods of *DHN* comprise single proton shuttling periods (Fig. 4f).

The observed differences between *FAD* and *DHN* can reasonably well be understood by considering the (zero temperature) energies and stabilities of the prototropic isomers, (*1*) = (*2*) and (*3*), and of the proton transfer transition states, (*1*↔*2*) and (*1*↔*3*) = (*2*↔*3*), (Figs. 1 and 2). For *FAD*, quantum chemical calculations yield the two equivalent minimum energy structures (*1*) and (*2*), and the D_{2h} symmetric double proton transfer transition state (*1*↔*2*) which is a saddle point (Table 1), whereas the single proton transfer product (*3*) is not a stationary state (*i.e.* is not a local minimum). Consequently and consistently, proton transfer processes (almost) exclusively take place by a concerted one-step mechanism that simultaneously involves both O–H$\cdot\cdot$O groups: (*1*)→(*1*↔*2*)→(*2*). What is more, single processes that involve only one O–H$\cdot\cdot$O group are almost exclusively restricted to concerted crossing-recrossing events where the proton undergoes a large amplitude vibration for just one cycle, which means that situations which

cause single proton activity are highly unstable and persist for very short time periods only.

With *DHN* the situation is distinctly different. Quantum chemical calculations show that besides the two global minima (*1*) and (*2*) the product of a single proton transfer reaction (*3*) is also a minimum on the PES (*i.e.* 4,8-*DHN* is a metastable tautomer), and the transition states for single proton transfer (*1*↔*3*) and (*2*↔*3*) are also saddle points (Table 2). What is more, at all levels of theory the energies of the different species increase within the series $(1) = (2) < (3) < (1 \leftrightarrow 3) = (2 \leftrightarrow 3) < (1 \leftrightarrow 2)$. Consequently, single proton transfer processes should be energetically preferred over (simultaneous) double proton transfer processes. Quite consistently, the majority of active processes observed within the PAW trajectories of *DHN* are single processes that are confined to only one O–H · · O group and involve the single proton transfer transition states $(1 \leftrightarrow 3) = (2 \leftrightarrow 3)$ and the metastable isomer (*3*): one- or two-step crossing-recrossing events, consecutive two-step double proton transfer processes, and single proton shuttling. In outstanding cases the meastable prototropic isomer (*3*) remains stable for more than 200 fs. On the other hand, because of the high energy of the double proton transfer transition state (*1*↔*2*), concerted double proton transfer or double proton shuttling processes are rather scarce.

Conclusions

The PAW molecular dynamics studies about proton motion and proton transfer in *FAD* and in *DHN* reported in this paper on the one hand largely confirm the results of a foregoing study on malonaldehyde [2, 3]. On the other hand, since the two compounds under consideration are capable of double proton transfer, the present study should further contribute to the understanding of these processes.

At first glance, within the PAW trajectories we can distinguish between normal and active periods. In the former case, a proton remains firmly attached at one oxygen atom, in the latter case a proton undergoes large amplitude motions between the two adjacent oxygen atoms which may (but not necessarily must) result in proton transfer. From a geometric point of view there exist no definite requirements for proton activity to occur, but on the average, within the active periods the R(O· · ·O) distances are distinctly shorter (by about 25 pm) than within the normal periods.

Within the active periods we find isolated transitions (one transition: O–H · · O → O · · H–O), crossing-recrossing events (two transitions: O–H · · O → O · · H–O → O–H · · O), and shuttling periods (several consecutive transitions: O–H · · O → O · · H–O → O–H · · O → O · · H–O → →). We also find single and double processes that involve only one or (simultaneously) both O · · H · · O groups respectively, and we can also distinguish between concerted one-step processes and successive two-step processes.

A reasonable and descriptive understanding of the driving forces behind the proton motion can be obtained by considering time evolutions of the potential that governs the motion of the proton between the two adjacent oxygen atoms. Normal periods are associated with asymmetric potentials with the minimum clearly located at one of the two oxygen atoms, as they are characteristic for normal,

clearly asymmetric O–H···O hydrogen bonds, whereas active periods are associated with broad, (near-)symmetric single- or double-minimum potentials, as they are characteristic for (near-)symmetric O···H···O hydrogen bonds.

An apparent difference between the two title compounds concerns the mechanism of double proton transitions. With *FAD* these are almost exclusively simultaneous one-step processes, whereas with *DHN* these are preferably two-step processes (*i.e.* two successive single proton transitions). This difference can reasonably well be attributed to the fact that single proton transfer in *DHN* yields the metastable 4,8-*DHN*, the energy of which is safely below the double proton transfer transition state, whereas with *FAD* the double proton transfer transition state is the only saddle point, and single proton transfer does not yield a metastable intermediate state.

Acknowledgements

The authors are grateful to Doz. *P. E. Blöchl*, IBM research division, Zürich (Switzerland), and to Dr. *E. Nusterer* and Prof. *K. Schwarz*, Technical University of Vienna (Austria) for valuable help and discussion. The work was supported by the *Jubiläumsfonds der Österreichischen Nationalbank*, Proj. No. 7237. Ample supply of computer facilities (IBM-RISC 6000/550 and Digital Alpha 2100 5/375) by the Computer Centre of the University of Vienna is kindly acknowledged.

References

[1] Blöchl PE (1994) Phys Chem Rev B **50**: 17953
[2] Wolf K, Mikenda W, Nusterer E, Schwarz K, Ulbricht C (1998) Chem Eur J **4**: 1418
[3] Wolf K, Mikenda W, Nusterer E, Schwarz K (1998) J Mol Struct **448**:201
[4] Car R, Parrinello M (1985) Phys Rev Lett **55**: 2471
[5] Mualem R, Sominska E, Kelner V, Gedanken A (1992) J Chem Phys **97**: 8813
[6] Marechal Y (1988) J Mol Struct **189**: 55
[7] Wachs T, Borchardt D, Bauer SH (1987) Spectrochim Acta A **43**: 965
[8] Bertie JE, Michaelian KH, Eysel HH, Hager D (1986) J Chem Phys **85**: 4779
[9] Bertie JE, Michaelian KH (1982) J Chem Phys **76**: 886
[10] Bournay J, Marechal Y (1975) Spectrochim Acta A **31**: 1351
[11] Rothschild WG (1974) J Chem Phys **61**: 3422
[12] Morita H, Nagakura S (1972) J Mol Spec **42**: 536
[13] Almenningen A, Bastiansen O, Motzfeld T (1969) Acta Chem Scand **23**: 2848
[14] Qian W, Krimm S (1998) J Phys Chem A **102**: 659
[15] Qian W, Krimm S (1998) J Phys Chem A **101**: 5825
[16] Wolfs I, Desseyn HO (1996) J Mol Struct (Theochem) **360**: 81
[17] Chojnacki H, Andzelm J, Nguyen DT, Sokalski WA (1995) Computers Chem **19**: 181
[18] Borisenko KB, Bock CW, Hargittai I (1995) J Mol Struct (Theochem) **332**: 161
[19] Chang YT, Yamaguchi Y, Miller WH, Schaefer HF III (1987) J Am Chem Soc **109**: 7245
[20] Mijoule C, Allavena M, Leclercq JM, Bouteiller Y (1986) Chem Phys **109**: 207
[21] Karpfen A (1984) Chem Phys **88**: 415
[22] Robertson GN, Lawrence MC (1981) Chem Phys **62**: 131
[23] Bosi P, Zerbi G, Clementi E (1977) J Chem Phys **66**: 3376
[24] Del Bene JE, Kochenour WL (1976) J Am Chem Soc **98**: 2041
[25] Lim JH, Lee EK, Kim Y (1997) J Phys Chem A **101**: 2233
[26] Jursic B (1997) J Mol Struct (Theochem) **417**: 89

[27] Chojnacki H (1997) Molecular Engineering **7**: 161
[28] Kim Y (1996) J Am Chem Soc **118**: 1522
[29] Shida N, Barbara PF, Almlöf J (1991) J Chem Phys **94**: 3633
[30] Hayashi S, Umemura J, Kato S, Morokuma K (1984) J Phys Chem **88**: 1330
[31] Graf F, Meyer R, Ha TK, Ernst RR (1981) J Chem Phys **75**: 2914
[32] Reynhardt EC (1992) Mol Phys **76**: 525
[33] Paul SO, Schutte CJH, Hendra PJ (1990) Spectrochim Acta A **46**: 323
[34] Olivieri A, Paul IC, Curtin DY (1990) Magn Res Chem **28**: 119
[35] Herbstein FH, Kapon M, Reisner GM, Lehman MS, Kress RB, Wilson RB, Shiau WI, Duesler EN, Paul IC, Curtin DY (1985) Proc R Soc Lond A **399**: 295
[36] Rentzepis PM, Bondybey VE (1984) J Chem Phys **80**: 4727
[37] Bondybey VE, Milton SV, English JH, Rentzepis PM, (1983) Chem Phys Lett **97**: 130
[38] Anoshin AN, Kopteva TS, Mikhailova KV, Shapiro IO, Shigorin DN (1982) Russ J Phys Chem **56**: 1215
[39] Shiau WI, Duesler EN, Paul IC, Curtin DY (1980) J Am Chem Soc **102**: 4546
[40] Bratan S, Strohbusch F (1980) J Mol Struct **61**: 409
[41] Ramondo F, Bencivenni L (1994) Struct Chem **5**: 211
[42] Schutte CJH, Paul SO, Smit R (1993) J Mol Struct **297**: 235
[43] Anoshin AN, Gastilovich EA, Mishenina KA (1983) Russ J Phys Chem **57**: 867
[44] Anoshin AN, Gastilovich EA, Nekrasov VV, Nurmukhametov RN, Shigorin DN (1983) Russ J Phys Chem **57**: 870
[45] De la Vega JR, Busch JH, Schauble JH, Kunze KL, Haggert BE (1982) J Am Chem Soc **104**: 3295
[46] Nosè S (1984) Mol Phys **52**: 255
[47] Hoover WG (1985) Phys Rev A **31**:1965
[48] Perdew JP, Zunger A (1981) Phys Rev B **23**: 5048
[49] Ceperley D, Alder BJ (1980) Phys Rev Lett **45**: 566
[50] Becke AD (1992) J Chem Phys **96**: 2155
[51] Perdew JP (1986) Phys Rev B **33**: 8822
[52] Frisch MJ, Trucks GW, Schlegel HB, Gill PMW, Johnson BG, Wong MW, Foresman JB, Rob MA, Head-Gordon M, Replogle ES, Gomperts R, Andres JL, Raghavahari K, Binkley JS, Gonzales C, Martin RL, Fox DJ, Defrees DJ, Baker J, Stewart JJP, Pople JA (1993) Gaussian 92, Rev G4. Gaussian, Inc, Pittsburgh, PA

Received November 13, 1998. Accepted (revised) January 12, 1999